

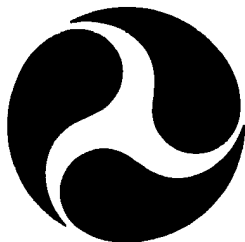
Report No. CG-D-27-95

ANALYSIS OF THE IIP ICEBERG DRIFT MODEL
Annex H of Cost and Operational Effectiveness Analysis for
Selected International Ice Patrol Mission Alternatives



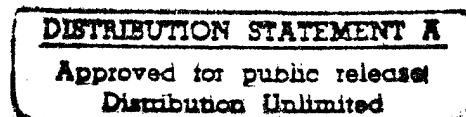
Robert L. Armacost

EER Systems Corporation
Vienna, VA



FINAL REPORT

JUNE 1995



This document is available to the U.S. public through the
National Technical Information Service, Springfield, Virginia 22161

Prepared for:

U.S. Coast Guard
Research and Development Center
1082 Shennecossett Road
Groton, Connecticut 06340-6096

and

U.S. Department Of Transportation
United States Coast Guard
Office of Engineering, Logistics, and Development
Washington, DC 20593-0001

19951024 171

DTIC QUALITY INSPECTED 8

NOTICE

This document is disseminated under the sponsorship of the Department of Transportation in the interest of information exchange. The United States Government assumes no liability for its contents or use thereof.

The United States Government does not endorse products or manufacturers. Trade or manufacturers' names appear herein solely because they are considered essential to the object of this report.

The contents of this report reflect the views of the Coast Guard Research & Development Center. This report does not constitute a standard, specification, or regulation.



G. T. Gunther
Technical Director, Acting
United States Coast Guard
Research & Development Center
1082 Shennecossett Road
Groton, CT 06340-6096

1. Report No. CG-D-27-95		2. Government Accession No.		3. Recipient's Catalog No.	
4. Title and Subtitle ANALYSIS OF THE IIP ICEBERG DRIFT MODEL Cost and Operational Effectiveness Analysis for Selected International Ice Patrol Mission Alternatives, Annex H				5. Report Date May, 1995	
				6. Performing Organization Code	
				8. Performing Organization Report No. R&DC 26/95	
7. Author(s) Armancost, Robert L.				10. Work Unit No. (TRAIS)	
9. Performing Organization Name and Address EER Systems Corporation 1593 Spring Hill Road Vienna, VA 22182				11. Contract or Grant No. DTCG39-94-C-E00085	
				13. Type of Report and Period Covered Final Report July, 1994 to June, 1995	
12. Sponsoring Agency Name and Address U.S. Department of Transportation U.S. Coast Guard Office of Engineering, Logistics, and Development Washington, DC 20593-0001 United States Coast Guard Research and Development Center 1082 Shennecossett Road Groton, CT 06340-6069				14. Sponsoring Agency Code	
15. Supplementary Notes					
16. Abstract <p>This report is Interim Report Volume 8 for the Cost and Operational Effectiveness Analysis for Ice Patrol Mission Analysis Study. The International Ice Patrol has developed a model of iceberg drift that plays a critical role in the overall modeling of iceberg locations and determining the Limits of All Known Ice. The drift model depends on the reported size of the iceberg and a number of environmental parameters. This report examines the structure of the drift model, reviews empirical evaluations of the model, and conducts an analytical and experimental sensitivity analysis of the model outputs with respect to the model parameters. The result of this analysis suggests that the local wind driven current portion of the deterioration model should be reexamined. The analyses indicate that the current speed magnitude is somewhat sensitive to errors in the wind speed that is provided as an input. Similar analyses with respect to errors in wind direction indicate that errors in wind direction may have a significant impact on estimated current direction. A comparison with a SAR current model yielded significantly different results. Before any current model changes are made based on the analysis of the SAR current model, the differences between the two models must be resolved. Other aspects of the drift model appear to provide a reasonable representation of the actual drift process. The analytical evaluation of the iceberg drift model reveals that there is little need for improved estimates of the environmental parameters for direct use in the drift model. The analysis illustrated the importance of correct classification. It is suggested that the current policy of classifying unknown icebergs as non-tabular medium icebergs be reexamined. Finally, the sensitivity of positional accuracy was clearly illustrated for the drift model. It is important to be able to improve the initial positioning accuracy to ensure that the probability of using the correct geostrophic current is maximized.</p>					
17. Key Words International Ice Patrol Icebergs Iceberg drift			18. Distribution Statement Document is available to the U.S. public through the National Technical Information Service Springfield, VA 22161		
19. Security Classif. (of this report) Unclassified		20. SECURITY CLASSIF. (of this page) Unclassified		21. No. of Pages 22	
				22. Price	

METRIC CONVERSION FACTORS

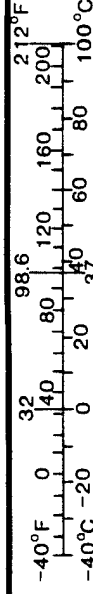
Approximate Conversions to Metric Measures

Symbol	When You Know	Multiply By	To Find	Symbol
LENGTH				
in	inches	* 2.5	centimeters	cm
ft	feet	30	centimeters	cm
yd	yards	0.9	meters	m
mi	miles	1.6	kilometers	km
AREA				
in ²	square inches	6.5	square centimeters	cm ²
ft ²	square feet	0.09	square meters	m ²
yd ²	square yards	0.8	square meters	m ²
mi ²	square miles	2.6	square kilometers	km ²
	acres	0.4	hectares	ha
MASS (WEIGHT)				
oz	ounces	28	grams	g
lb	pounds	0.45	kilograms	kg
	short tons (2000 lb)	0.9	tonnes	t
VOLUME				
tsp	teaspoons	5	milliliters	ml
tbsp	tablespoons	15	milliliters	ml
fl oz	fluid ounces	30	milliliters	ml
c	cups	0.24	liters	l
pt	pints	0.47	liters	l
qt	quarts	0.95	liters	l
gal	gallons	3.8	liters	l
ft ³	cubic feet	0.03	cubic meters	m ³
yd ³	cubic yards	0.76	cubic meters	m ³
TEMPERATURE (EXACT)				
°F	Fahrenheit temperature	5/9 (after subtracting 32)	Celsius temperature	°C

*1 in = 2.54 (exactly).

Approximate Conversions from Metric Measures

Symbol	When You Know	Multiply By	To Find	Symbol
LENGTH				
mm	millimeters	0.04	inches	in
cm	centimeters	0.4	inches	in
m	meters	3.3	feet	ft
m	meters	1.1	yards	yd
km	kilometers	0.6	miles	mi
AREA				
cm ²	square centimeters	0.16	square inches	in ²
m ²	square meters	1.2	square yards	yd ²
km ²	square kilometers	0.4	square miles	mi ²
ha	hectares (10,000 m ²)	2.5	acres	
MASS (WEIGHT)				
g	grams	0.035	ounces	oz
kg	kilograms	2.2	pounds	lb
t	tonnes (1000 kg)	1.1	short tons	
VOLUME				
ml	milliliters	0.03	fluid ounces	fl oz
l	liters	0.125	cups	c
l	liters	2.1	pints	pt
l	liters	1.06	quarts	qt
l	liters	0.26	gallons	gal
m ³	cubic meters	35	cubic feet	ft ³
m ³	cubic meters	1.3	cubic yards	yd ³
TEMPERATURE (EXACT)				
°C	Celsius temperature	9/5 (then add 32)	Fahrenheit temperature	°F



ANALYSIS OF THE IIP ICEBERG DRIFT MODEL

ABSTRACT

The International Ice Patrol has developed a model of iceberg drift that plays a critical role in the overall modeling of iceberg locations and determining the Limits of All Known Ice. The drift model, along with an iceberg deterioration model, is used to determine the location and state of any reported iceberg until it is resighted. The drift model depends on the reported size of the iceberg and a number of environmental parameters. This report examines the structure of the drift model, reviews empirical evaluations of the model, and conducts an analytical and experimental sensitivity analysis of the model outputs with respect to the model parameters. The result of this analysis suggests that the local wind driven current portion of the deterioration model should be reexamined. The analyses indicate that the current speed magnitude is somewhat sensitive to errors in the wind speed that is provided as an input. Similar analyses with respect to errors in wind direction indicate that errors in wind direction may have a significant impact on estimated current direction. A comparison with a SAR current model yielded significantly different results. Before any current model changes are made based on the analysis of the SAR current model, the differences between the two models must be resolved. Other aspects of the drift model appear to provide a reasonable representation of the actual drift process. The analytical evaluation of the iceberg drift model reveals that there is little need for improved estimates of the environmental parameters for direct use in the drift model. The analysis illustrated the importance of correct classification. It is suggested that the current policy of classifying unknown icebergs as non-tabular medium icebergs be reexamined. Finally, the sensitivity of positional accuracy was clearly illustrated for the drift model. It is important to be able to improve the initial positioning accuracy to ensure that the probability of using the correct geostrophic current is maximized.

INTRODUCTION

Objective.

The IIP uses an Iceberg Drift Model to emulate the approximate drift behavior of icebergs in the presence of known environmental conditions. The results of this model along with those from the iceberg deterioration model result in a description of the location and melt state of icebergs that is used to determine the Limits of All Known Ice (LAKI). The selected modeling alternatives for Phase II of the Cost and Operational

A-1

<input checked="checked" type="checkbox"/>
<input type="checkbox"/>
<input type="checkbox"/>
Codes
nd / or cial

Effectiveness Analysis included conducting a detailed sensitivity analysis of the deterioration and drift models and developing an approach to characterize the risk posture for the IIP (Armcast, 1994). The detailed sensitivity analysis of the deterioration model and the development of a risk model are addressed in other reports. The purpose of this report is to review the structure of the existing model and to examine the sensitivity of its output with respect to changes in input parameters. This analysis identifies which input parameters require the most attention with respect to accuracy of their estimates and identifies areas where potential model enhancements are appropriate.

Background.

The iceberg drift model used by IIP was completed and tested in 1980 (Mountain, 1980). Its format and use remains essentially the same to date. The fundamental drift model balance is between iceberg acceleration, air and water drag, the Coriolis acceleration and a sea surface slope term characterized by the mean ocean currents. The resulting differential equations are solved using a fourth-order Runge-Kutta analysis. Key input data include: iceberg location; iceberg size and shape; local wind; geostrophic (mean) current; and local currents from drift buoys.

Sensed or sighted icebergs are placed into one of four size categories (growler, small, medium, and large with no upper limit) which also automatically sets the mass and cross-sectional areas to the assumed characteristic values for the designated size category. One of two specific shape classifications, tabular or non-tabular, is also made when a visual sighting occurs. The model divides the subsurface shape of the iceberg into up to four draft layers, each with its own cross sectional size, depending on the iceberg classification. These areas are affected by the geostrophic ocean water current and a calculated depth and time dependent local wind driven current. A separate model is used to estimate the local wind driven current (Mooney, 1978, Mountain and Mooney, 1979). Icebergs whose size are unknown are assumed to be medium icebergs; those whose shape are unknown are assumed to be non-tabular icebergs. The model is operated every 12 hours using the most recent wind data, and drifts all icebergs on plot within the IIP operations area.

The IIP estimates that the initial position error is 5 nm regardless of sighting source and that model drift error increases linearly in 5 nautical mile per day increments for each 24 hours of additional model drift up to a maximum radius of 30 nautical miles. This maximum error of 30 nautical miles occurs after 5 days of drift. There is no increase in the maximum 30 nautical mile error estimate regardless of how long the iceberg is drifted within the IIP operations area. If an iceberg is resighted, the drift error calculation is restarted. Icebergs south of 40°N are assumed to have a daily drift error of 10 nm, accumulating over a period of 5 days to a maximum error of 55 nm.

Iceberg Drift Model.

The Iceberg Drift Model (Mountain, 1980) is comprised of a set of four differential equations that balance iceberg acceleration with the forces associated with air and water drag, the Coriolis acceleration and a sea surface slope term which describes the mean ocean currents. The equations of motion for the drift of an iceberg in component form are:

$$\frac{dx}{dt} = U \quad (1)$$

$$\frac{dy}{dt} = V \quad (2)$$

$$\frac{dU}{dt} = fV - fV_g + [1/2\rho_a CD_a A_a W^2 \sin \theta + \sum_{i=1}^4 1/2\rho_w CD_w A_i (E_i - U)S_i] / M \quad (3)$$

$$\frac{dV}{dt} = fU - fU_g + [1/2\rho_a CD_a A_a W^2 \cos \theta + \sum_{i=1}^4 1/2\rho_w CD_w A_i (N_i - V)S_i] / M \quad (4)$$

where

- x, y = east, north components of position
- U, V = east, north components of iceberg velocity
- U_g, V_g = east, north components of mean (geostrophic) water velocity
- U_{E_i}, V_{E_i} = east, north components of Ekman current in i th layer
- E_i = $U_g + U_{E_i}$, east component of total water current in i th layer
- N_i = $V_g + V_{E_i}$, north component of total water current in i th layer
- S_i = $[(E_i - U)^2 + (N_i - V)^2]^{1/2}$, speed of iceberg relative to i th layer
- A_a = iceberg cross sectional area above the water
- A_i = iceberg cross sectional area in the i th layer
- f = the Coriolis parameter
- M = the iceberg mass
- W = wind speed
- θ = wind direction
- CD_a, CD_w = drag coefficient in air, water
- ρ_a, ρ_w = density of air, water

Equations (1)-(4) are solved using a fourth order Runge-Kutta method to obtain the east and north components of the iceberg drift.

The Ekman current components are obtained using a local wind driven current model (Mooney, 1978; Mountain and Mooney, 1979) that uses a 96 hour wind history. The IIP implementation uses eight 12 hour periods. The model from Mountain and Mooney (1979) involves two equations that are applied at each layer:

$$U_{E_i} = \sum_{k=1}^8 K_k F_k \sin(\theta_k - \phi_k) \quad (5)$$

$$V_{E_i} = \sum_{k=1}^8 K_k F_k \cos(\theta_k - \varphi_k) \quad (6)$$

where

- F_k = magnitude of wind stress during the k th interval
- θ_k = direction of wind stress during the k th interval
- K_k, φ_k = constants affecting the magnitude and rotation of the current in k th interval

The local wind driven current speed and direction are given as:

$$\text{Current speed} = \sqrt{U_{E_i}^2 + V_{E_i}^2} \quad (7)$$

$$\text{Current direction} = \tan^{-1}(U_{E_i} / V_{E_i}) \quad (8)$$

Mountain and Mooney (1979) present selected values of K_k, φ_k for sixteen six-hour time intervals (covers a 96-hour time history) and selected latitudes. The IIP implementation utilizes base values for 45°N and adjusts for other latitudes using a gradient approach. The IIP implementation uses eight twelve-hour time intervals to cover the 96-hour time history of local wind. Mountain and Mooney do not specify how the wind stress, F_k , is to be computed. In Mooney's (1978) development, the wind stress is linearly dependent on the wind speed, $F_k = \rho_a C_D W$. In a review of the Mooney model, Dick (1991) noted that many oceanographers use a quadratic relationship, $F_k = \rho_a C_D W^2$. Despite the linear model in Mooney's formulation, the IIP implementation does use the quadratic form to estimate wind stress (lines 49 and 50 in SUBROUTINE NEWWIND).

QUALITATIVE AND EMPIRICAL EVALUATION OF THE MODEL

Initial model tests in 1980 used the tracks of 2 large tabular icebergs, a large pinnacle iceberg, and a freely drifting satellite-tracked buoy to compare the model performance with actual iceberg drift (Mountain, 1980). Results ranged from approximately a 5 nautical mile error for a 3 day drift to a constant 50-80 nautical mile error in the 25 day case. The assumed cause for the error in this test was stated to be inaccurate wind and current data inputs to the model.

In 1985, drift model tests were held in several different parts of the IIP operations area (Murphy and Anderson, 1985). Four case studies were performed using the drift model. In 3 of the 4 cases, the drift of the icebergs as depicted by the model using the system data had location errors ranging from 40 nautical miles after a 2.5 day drift, 30 nautical miles after a 3.3 day drift, and 45 nautical miles after a 4 day drift. These all exceed the standard drift error assumed by the IIP of a maximum of 30 nautical miles after a drift of 5 days. The 4th case study drift did remain well within the standard drift error

and did not exceed an error of more than approximately 11 nautical miles over a 4 day drift. Better performance results from the model were realized when using the observed current and wind data for all four case studies, instead of the automatically provided system data. (It is not known whether current from the local wind driven current was used at the different iceberg layers.) However, even with using real time data, in only one case was the predicted iceberg drift position error well within the accepted limits. Projecting a drift experiment such as this for a total period of 2 weeks, or 3 times as long as these case studies, suggests that the drift errors would continue to generate and become even larger.

Using the on scene wind and current data resulted in estimated positions closer to the actual iceberg position than using geostrophic currents and FNMOC winds. The limited experiments suggest that the structure of the model is sound and that its accuracy depends on the accuracy of the input data. The experiments did not isolate wind or current as the primary causal factor in generating errors. However, the case of one iceberg in Murphy and Anderson (1985) showed significant improvement by using observed currents with FNMOC winds. It should be noted that three of the cases in the Murphy and Anderson (1985) experiment were located in areas where significant reductions in geostrophic currents were instituted in 1989-90 (Murphy, Hanson, and Tuxhorn, 1990). It is also important to note that based on the trends in the various drift results, if the tests were continued beyond the 4 days, the model error would likely exceed the 30 nautical miles maximum drift error after a period of 10 days of predictions even with using the best on scene, observed data available. In practice, it is not known to what extent positional errors affect the overall accuracy of the predicted positions.

ANALYTICAL EVALUATION OF THE ICEBERG DETERIORATION MODEL

In analyzing the drift model, it is appropriate to separately analyze the local wind driven (Ekman) current model separately, and then evaluate the overall drift model.

Local Wind Driven Current Model.

Analytical Analysis.

The east component of the local wind driven current is given as follows:

$$U_{E_i} = \sum_{k=1}^8 K_k \rho_w CD_w W_k^2 \sin(\theta_k - \phi_k) \quad (9)$$

The input variables are the wind speed and direction. The first order sensitivity of the current speed with respect to the inputs is given by the partial derivatives as follows:

$$\frac{\partial U_{E_i}}{\partial W_k} = 2\rho_w CD_w W_k \sin(\theta_k - \phi_k) \quad (10)$$

$$\text{and } \frac{\partial U_{E_i}}{\partial \theta_k} = \rho_w CD_w W_k^2 \cos(\theta_k - \varphi_k). \quad (11)$$

Similar partial derivatives can be obtained for the north component of the local wind driven current. With respect to local wind speed, the change in the east and north components varies with the wind speed and greater increases (or overestimates of wind speed) will have a greater effect. With respect to wind direction, the effect of changes varies as the cosine of the angular error. Unfortunately, it is virtually impossible to analytically determine what the impact will be on the resulting current. The changes represented by equations (10) and (11) are for the k th time interval. The total impact of changes or data errors over all time intervals is incorporated in the sum in equation (9) for the east component and in equation (6) for the north component. The overall effect on current speed and direction is finally reflected in equations (7) and (8). The derivative of current speed is easily obtained and indicates that it varies linearly with the wind speed and proportional to the cosine of the wind direction error. The derivative with respect to wind direction can also be obtained, but does not provide any immediate insight into how the current direction is affected by input data errors. Clearly, this requires an empirical sensitivity analysis to identify these effects.

Empirical Analysis.

There are three models for local wind driven current that are available. Mooney's (1978) model uses a linear relationship for wind stress. It includes a table of eight values for (K_k, φ_k) corresponding to six-hour increments of wind information and an eddy viscosity of 50 cm²/sec for latitudes ranging from 0° to 65°N in 5° increments. Mountain and Mooney's (1979) model does not specify how wind stress is computed. It includes a table of sixteen values for (K_k, φ_k) corresponding to six-hour increments of wind information and an eddy viscosity of 100 and 500 cm²/sec for latitudes at 25° and 50°N for surface currents and the current at 20m. The third model is the one that is coded in the IIP computer software and used in the DMPS model. The current code is extracted from SUBROUTINE NEWWIND in Figure 1.

The IIP drift model as extracted from Figure 1 and using the surface current Ekman parameters from SUBROUTINE NEWWIND at 45°N latitude was modeled in an Excel spreadsheet. Nominal wind speed was 20 knots and the wind was from the south (180°). Assuming that this wind was constant over 96 hours, the resulting local wind driven current at the surface is 10.287 cm/sec (0.2 knots) at 086° using the IIP drift model. The detailed results are included in Appendix I.

The primary focus here is the effect on the local wind driven current when there are errors or perturbations in the input wind speed and direction. These effects were examined jointly considering a 10% change in wind speed (± 2 knots) and a 15° change in wind direction. The effect on current speed is indicated in Table 1.

```

DO 20 I=1,4
  EKX(I) = 0.0
  EKY(I) = 0.0
20 CONTINUE
IN = ITIME - 7
DO 40 JT = IN,ITIME
  ILAG = JT - IN + 1
  WNDSPD=IWDATA(IW,JW,JT)/100
  WINDDIR=(IWDATA(IW,JW,JT)-IWDATA(IW,JW,JT)/100)*100*10
  WNDSPQUAR=WNDSPD*WNDSPD*2642.0
  STRESS=ADC*AIRDNSTY*WINDSPQUAR (ADC=.0015; AIRDNSTY=.00125)
  DO 30 L = 1,ISIZE
    ROTA = ROT(ILAG,L)+(ALAT-45,0)*GRDR(ILAG,L)
    DEK = DK(ILAG,L)+(ALAT-45,0)*GRDK(ILAG,L)
    WIND = (WINDDIR+ROTA)*0.017452925
    EKX(L) = EKX(L) + DEK*STRESS*DSIN(WIND)
    EKY(L) = EKY(L) + DEK*STRESS*DCOS(WIND)
  30 CONTINUE
40 CONTINUE

```

Figure 1. Local wind driven current coding, SUBROUTINE NEWWIND.

Table 1. Effect on current speed with wind speed and direction perturbations.

Current Speed (cm/sec)				
Wind direction (degrees)				
Wind speed (kts)	165	180	195	% change
18	8.333	8.333	8.333	-19%
20	10.287	10.287	10.287	—
22	12.477	12.447	12.447	21%

As expected from the analytical results, changes in wind direction do not have any effect on current speed. Changes in wind speed, however, do have an effect on current speed. In this case, a 10% change in wind speed has approximately a 20% change in current speed. The same results hold if the nominal wind speed is increased to 40 knots and a 10% perturbation is effected.

A percentage perturbation makes little sense with respect to direction. Instead, the effects of a $\pm 15^\circ$ change was examined. The results are included in Table 2.

As indicated in the analytical section, there is little insight provided by the equations. The empirical results demonstrate that changes in the wind speed do not affect the current direction **when** the wind is *constant over the period*. (The *W* term factors out of the east and north components and does not affect the arctangent computation.) What is interesting in this analysis is how the current direction changes. In particular changing from a wind direction of 180° to 195° results in a 165° shift in the current direction. The

15° decrease in the wind direction results in a 15° decrease in current direction. At this point, there is no obvious explanation for this counterintuitive result.

Table 2. Effect on current speed with wind speed and direction perturbations.

Current Direction (degrees)			
Wind direction (degrees)			
Wind speed (kts)	165	180	195
18	71.2	86.2	-78.8
20	71.2	86.2	-78.8
22	71.2	86.2	-78.8
% change	-17%	--	-191%

Dick's (1991) Evaluation.

Recently, Dick (1991) prepared an Interim Report on an ongoing evaluation of the Mooney (1978) model as used for Search and Rescue (SAR) planning. She compared the SAR-Mooney model with a one-dimensional version of the mixed layer model developed by Mellor and Yamada (1982) and found that the SAR-Mooney model was inconsistent. For comparison purposes, the IIP drift model was exercised and the comparative results are in Table 3.

Table 3. Comparative drift model results.

Wind Speed m/s	Mellor-Yamada		SAR-Mooney		IIP-Mooney	
	Current m/s	Direction	Current m/s	Direction	Current m/s	Direction
2.5	0.01	76	0.04	48	0.006	86
5.0	0.03	76	0.08	48	0.022	86
10.0	0.08	59	0.15	48	0.097	86
20.0	0.20	49	0.30	48	0.389	86
40.0	0.47	43	0.60	48	1.557	86

The results in Table 3 indicate that none of the models agree. For low wind speeds, the IIP-Mooney model is much closer to the Mellor-Yamada model, but at high wind speeds, it diverges rapidly. A very interesting result is the difference between the SAR-Mooney model and the IIP-Mooney current model. Apparently, there are two different implementations.

Dick(1991) included some preliminary recommendations (pending completion of the analysis) that the SAR-Mooney model be replaced by a more accurate model for SAR and iceberg drift purposes. If, in fact, the Mellor-Yamada model is state-of-the-art, the above comparison suggests that the IIP-Mooney model may be overestimating local wind driven current velocity. This will increase the inaccuracy of the iceberg drift, but it is impossible to identify the direction of the error.

Summary.

The local wind driven current model is an important element of the iceberg drift model. The analytical and empirical analyses indicate that the current speed magnitude is somewhat sensitive to errors in the wind speed that is provided as an input. Similar analyses with respect to errors in wind direction indicate that errors in wind direction may have a significant impact on estimated current direction. Other comparisons with a SAR current model suggest that it should be replaced. The IIP current model, based on the same foundation as the SAR current model, yields significantly different results. Before any current model changes are made based on the analysis of the SAR current model, the differences between the two models must be resolved.

Main Drift Model.

The main variables/parameters that affect the drift model in equations (1)-(4) are environmental parameters (wind speed and direction), geostrophic current, and iceberg size and shape. The interaction among these parameters determines how the estimated drift will vary.

Environmental Parameters.

The sensitivity results from the local wind driven current model obviously affect the solution of equations (1)-(4). The wind speed and direction also impact equations (3) and (4) with respect to the above water area of the iceberg. The partial derivatives of this portion of the equation will be identical to equations (10)-(11) with the water parameters replaced by the corresponding air parameters. In equations (3) and (4), the drag coefficient of the iceberg in air is 0.0015 and in water is 0.8 (in the latest version of the code). The density of air is 0.00125. Assuming that the wind speed is ten times as great as the current speed, the weighting factor for the air wind stress is $(.00125 * .0015 * 100 = .0001875)$ compared with water current stress value of $(1 * 0.8 * 1 = 0.8)$. The impact of the water force is over 4,000 times as great as the air stress, assuming equal areas. Based on this analysis, the environmental parameters, except for the development of the local wind driven current, have little direct impact on iceberg drift.

Iceberg Classification.

The iceberg classification regarding size (growler, small, medium, large) and type (tabular, pinnacled) determines the surface areas and the iceberg mass used in equations (3) and (4). Mountain (1980) provided values for these parameters (see Table 1 in Mountain (1980)). Those values are currently used with the exception of growlers. Current parameters for growlers is $M = 9.6 \times 10^6 \text{ kg}$, $A_a = 57 \text{ m}^2$, and $A_l = 414 \text{ m}^2$.

To explore the impact of iceberg size selection on drift model results, we have computed the ratio of the iceberg area (above the water and the four segments below the

water) to the iceberg mass (A_i / M). This factor appears in each term in equations (3) and (4). As discussed above, assume that the forces on the dry area have negligible impact because of the density differences. Further, assume that the current at all levels is the same (speed and direction) and is equal to one speed unit. Then the "current contribution" in equations (3) and (4) is given in the last column of Table 4.

Table. 4. Iceberg Area/Mass ratio.

	Dry	0-20m	20-50m	50-100m	100-120m	Current Contribution
Non-Tabular						
Growler	5.94	43.13	0.00	0.00	0.00	43.13
Small	3.07	10.40	10.93	0.00	0.00	21.33
Medium	1.01	2.00	2.11	3.00	0.00	7.11
Large	0.36	0.64	0.68	0.96	0.25	2.54
Tabular						
Small	2.65	7.76	10.61	0.00	0.00	18.37
Medium	1.24	2.03	2.72	4.01	0.00	8.76
Large	0.63	0.87	1.18	1.75	0.61	4.41

The "current contributions" in Table 4 contribute to the acceleration of the iceberg and when equations (1)-(4) are solved will result in those with greater accelerations having greater velocity. The values in Table 4 satisfy our intuition that other things being equal, smaller icebergs will drift faster than larger icebergs. The data in Table 4 seem to suggest that larger tabular icebergs will drift faster than corresponding non-tabular icebergs whereas smaller non-tabular icebergs will drift faster than smaller tabular icebergs. The present policy assumes that an iceberg is a medium, non-tabular iceberg if a positive classification can not be made. Although this appears to be a conservative policy, the "current contribution" is almost three times as great for the medium iceberg as compared with the large (non-tabular) iceberg. None of the experiments to date have attempted to identify possible effects of misclassification.

Geostrophic Currents and Positional Accuracy.

Finally, the last input that impacts the solution of equations (1)-(4) is the geostrophic current. Because the geostrophic current is an average of past observations, it is inherently accurate as to its intended representation. The degree to which it corresponds to actual current is unknown in real time except for those cases where drift buoys are available. In fact, the drift buoys are used to provide a replacement for the geostrophic currents when real time drift buoy current data is available. Accuracy in geostrophic data used in the drift model is very dependent on positional accuracy.

To examine the impact of positional accuracy, we would like to estimate the probability that an iceberg is actually located in the area for which a geostrophic current is selected. The geostrophic current file is developed on a 20 second grid. Assume that the geostrophic current in adjacent north/south grids is approximately the same, but that

east/west grids may have significant differences, particularly with regard to current speed. The IIP assumes that the initial error in sighting an iceberg is 10 nm on the first day, increasing by 5 nm per day up to a maximum error of 30 nm. This error distribution is normally represented as a bivariate normal distribution and the "maximum" error corresponds to 3σ the range from -3σ to $+3\sigma$ covers 99.7% of possible locations. Under these conditions, we can assume that the marginal density of location across lines of longitude is normally distributed, and with the maximum error of 30 nm, $\sigma = 10$ nm. In the following, we develop a general model that can be used to estimate the probability of interest.

Assume that the grid size is d and that a perpendicular across the grid is divided into n segments, each of length d/n as illustrated in Figure 2. Assume further, that an iceberg position can be selected at any point in a given segment i . For ease of computation, we assume that this position is at the mid-point of the segment. Its value is easily computed as $\mu = (2i - 1)d / (2n)$ where i is the segment number (1 to n). Assume that the error in position is normally distributed with mean equal to the mid-point of an arbitrary segment and standard deviation equal to σ .

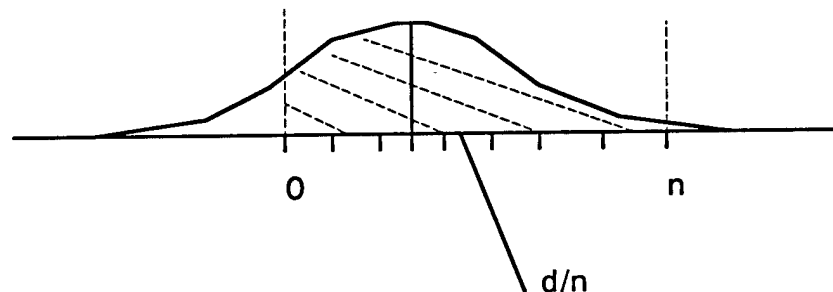


Figure 2. Estimation of positional accuracy.

The endpoints of the interval are easily computed as $z_L = -(2i - 1)d / (2n\sigma)$ and $z_U = [d - ((2i - 1)d / (2n))] / \sigma$ and the conditional probability is easily obtained from tables. The resulting probability is conditional with respect to the given segment. Assuming that each segment in the interval of width d is equally likely, the unconditional probability that the iceberg is in the given interval of width d is the simple average of the segment probabilities.

In the present case, $d = 20$ nm and $\sigma = 30$ nm. With ± 30 nm error, an easy estimate of the probability is $1/3$. Applying the above model, yields a probability of 0.61 that given a position of an iceberg is estimated in a given interval, it is actually there. This amounts to the probability that the correct geostrophic current is selected. The results for various allowed drift errors are included in Table 5.

Table 5 provides some insight into the potential benefits of improving the position estimation of the icebergs. In particular, if the initial position is much more accurate, for example, within 3 nm, the probability that one will select the correct geostrophic current

increases to 0.97. With the correct current, there is a much higher probability that the position at the next update will be correct and that the correct values of the geostrophic current will be used in equations (3) and (4).

Table 5. Probability of selecting correct geostrophic current using temporal error estimates.

Day	Error	Probability
1	10 nm	.87
2	15 nm	.80
3	20 nm	.74
4	25 nm	.67
5	30 nm	.61

Summary.

The analytical evaluation of the iceberg drift model reveals that there is little need for improved estimates of the environmental parameters for direct use in the drift model. The analysis illustrated the importance of correct classification. It is suggested that the current policy of classifying unknown icebergs as non-tabular medium icebergs be reexamined. Finally, the sensitivity of positional accuracy was clearly illustrated for the drift model. It is important to be able to improve the initial positioning accuracy to ensure that the probability of using the correct geostrophic current is maximized.

SUMMARY AND CONCLUSIONS

This evaluation and analysis of the IIP iceberg drift model has concluded that the model appears to be a very reasonable representation of the drift process. This conclusion is supported by our review and limited empirical data. However, it appears that the submodel providing the local wind driven current should be revisited. The inconsistencies in the drift results using three supposedly comparable models strongly suggests that the reasons for the differences be explained. The policy of characterizing unidentified icebergs as non-tabular medium icebergs should also be revisited. The total area to mass ratio suggests that a slower drift may be desirable. Such a review has to be taken in conjunction with other policy implications for the model (e.g., deterioration model). The analysis highlighted the critical importance of improving the accuracy of estimated iceberg positions. The flow through of this source of uncertainty should be examined in a simulation model when the local wind driven current model questions are resolved.

REFERENCES

- Armacost, R. L., 1994, *Interim Report on the Identification of Alternatives for Phase II Cost and Operational Effectiveness Analysis*, EER Systems Corporation, November.
- Armacost, R. L., Jacob, R. F., Kollmeyer, R. C., and Super, A. D., 1994, *Interim Report on the Analysis of Current Operations of the International Ice Patrol*, EER Systems Corporation, November.
- Dick, J. E., 1991, *Evaluation of Search and Rescue (SAR) Method for Determining Local Wind Current*, U.S. Coast Guard Report CG-D-07-92.
- Mooney, K. A., 1978, *A Method for Calculating the Local Wind Current*, U.S. Coast Guard, Oceanographic Unit Technical Report 78-2.
- Mountain, D. G., 1980, "On Predicting Iceberg Drift," *Cold Regions Science and Technology*, Vol. 1., No. 3/4, pp. 273-282.
- Mountain, D. G. and K. A. Mooney, 1979, "A Techniques for the Calculation of Time Dependent Wind Driven Currents," *Ocean Engineering*, Vol. 6, 541-547.
- Murphy, D. L. and I. Anderson, 1985, "International Ice Patrol Iceberg Sighting Data Base 1960-1991," Appendix D in *Report of the International Ice Patrol in the North Atlantic*, Bulletin No. 71, 1985 Season, CG-188-40, Washington, DC.
- Murphy, Donald L., Walter E. Hanson, and Ross L. Tuxhorn, 1990, "Modifications to Ice Patrol's Mean Current Data Base," Appendix C in *Report of the International Ice Patrol in the North Atlantic*, Bulletin No. 76, 1990 Season, CG-188-45, Washington, DC.

[BLANK]

Appendix I. Local Wind Driven Current Data Analysis.

This Appendix includes an analysis of the sensitivity of the local wind driven current speed and direction in the face of perturbations of the values of wind speed and wind direction. The models implement the current version of the local wind driven current model developed by Mooney (1978) and implemented by the International Ice Patrol.

Surface Layer								
t	Ft	Stress	theta-t	Kt	phi-t	th+phi-t	Ut	Vt
	kts		deg		deg	rad	cm/s	cm/s
1	20	1.9815	180	1.51	-68.4	1.94779	2.7819517	-1.101
2	20	1.9815	180	1.62	36	3.76991	-1.8868083	-2.597
3	20	1.9815	180	1.76	140.4	5.59203	-2.2229779	2.6871
4	20	1.9815	180	1.94	-115.4	1.12748	3.4725202	1.6489
5	20	1.9815	180	2.19	-11.7	2.93739	0.8799924	-4.249
6	20	1.9815	180	2.54	91.3	4.73508	-5.0317146	0.1142
7	20	1.9815	180	3.29	192	6.49262	1.3554044	6.3767
8	20	1.9815	180	5.62	281.4	8.05295	10.916329	-2.201
sum							10.264697	0.678
							v=	10.287
angle(deg)								86.221

Surface Layer								
t	Ft	Stress	theta-t	Kt	phi-t	th+phi-t	Ut	Vt
	kts		deg		deg	rad	cm/s	cm/s
1	18	1.605015	180	1.51	-68.4	1.94779	2.2533809	-0.892
2	18	1.605015	180	1.62	36	3.76991	-1.5283147	-2.104
3	18	1.605015	180	1.76	140.4	5.59203	-1.8006121	2.1766
4	18	1.605015	180	1.94	-115.4	1.12748	2.8127414	1.3356
5	18	1.605015	180	2.19	-11.7	2.93739	0.7127939	-3.442
6	18	1.605015	180	2.54	91.3	4.73508	-4.0756888	0.0925
7	18	1.605015	180	3.29	192	6.49262	1.0978775	5.1651
8	18	1.605015	180	5.62	281.4	8.05295	8.8422267	-1.783
sum							8.3144047	0.5492
							v=	8.3325
angle(deg)								86.221

Surface Layer								
t	Ft	Stress	theta-t	Kt	phi-t	th+phi-t	Ut	Vt
	kts		deg		deg	rad	cm/s	cm/s
1	22	2.397615	180	1.51	-68.4	1.94779	3.3661615	-1.333
2	22	2.397615	180	1.62	36	3.76991	-2.283038	-3.142
3	22	2.397615	180	1.76	140.4	5.59203	-2.6898033	3.2514
4	22	2.397615	180	1.94	-115.4	1.12748	4.2017495	1.9951
5	22	2.397615	180	2.19	-11.7	2.93739	1.0647908	-5.142
6	22	2.397615	180	2.54	91.3	4.73508	-6.0883746	0.1382
7	22	2.397615	180	3.29	192	6.49262	1.6400393	7.7158
8	22	2.397615	180	5.62	281.4	8.05295	13.208758	-2.663
sum							12.420284	0.8204
							v=	12.447
angle(deg)								86.221

Figure I-1. Local wind driven current, 10% speed perturbation at 180° direction.

Surface Layer								
t	Ft	Stress	theta-t	Kt	phi-t	th+phi-t	Ut	Vt
	kts		deg		deg	rad	cm/s	cm/s
1	20	1.9815	165	1.51	-68.4	1.68599	2.9722359	-0.344
2	20	1.9815	165	1.62	36	3.50811	-1.1503719	-2.997
3	20	1.9815	165	1.76	140.4	5.33024	-2.8427093	2.0202
4	20	1.9815	165	1.94	-115.4	0.86568	2.927437	2.4914
5	20	1.9815	165	2.19	-11.7	2.67559	1.9498131	-3.877
6	20	1.9815	165	2.54	91.3	4.47328	-4.8898164	-1.192
7	20	1.9815	165	3.29	192	6.23083	-0.3411852	6.5102
8	20	1.9815	165	5.62	281.4	7.79115	11.114056	0.6992
sum							9.7394588	3.3116
							v=	10.287
angle(deg)								71.221

Surface Layer								
t	Ft	Stress	theta-t	Kt	phi-t	th+phi-t	Ut	Vt
	kts		deg		deg	rad	cm/s	cm/s
1	18	1.605015	165	1.51	-68.4	1.68599	2.4075111	-0.279
2	18	1.605015	165	1.62	36	3.50811	-0.9318012	-2.427
3	18	1.605015	165	1.76	140.4	5.33024	-2.3025945	1.6364
4	18	1.605015	165	1.94	-115.4	0.86568	2.371224	2.0181
5	18	1.605015	165	2.19	-11.7	2.67559	1.5793486	-3.14
6	18	1.605015	165	2.54	91.3	4.47328	-3.9607513	-0.966
7	18	1.605015	165	3.29	192	6.23083	-0.27636	5.2733
8	18	1.605015	165	5.62	281.4	7.79115	9.002385	0.5664
sum							7.8889616	2.6824
							v=	8.3325
angle(deg)								71.221

Surface Layer								
t	Ft	Stress	theta-t	Kt	phi-t	th+phi-t	Ut	Vt
	kts		deg		deg	rad	cm/s	cm/s
1	22	2.397615	165	1.51	-68.4	1.68599	3.5964054	-0.416
2	22	2.397615	165	1.62	36	3.50811	-1.39195	-3.626
3	22	2.397615	165	1.76	140.4	5.33024	-3.4396782	2.4445
4	22	2.397615	165	1.94	-115.4	0.86568	3.5421988	3.0146
5	22	2.397615	165	2.19	-11.7	2.67559	2.3592738	-4.691
6	22	2.397615	165	2.54	91.3	4.47328	-5.9166779	-1.442
7	22	2.397615	165	3.29	192	6.23083	-0.412834	7.8773
8	22	2.397615	165	5.62	281.4	7.79115	13.448007	0.8461
sum							11.784745	4.007
							v=	12.447
angle(deg)								71.221

Figure I-2. Local wind driven current, 10% speed perturbation at -15° direction.

Surface Layer								
t	Ft	Stress	theta-t	Kt	phi-t	th+phi-t	Ut	Vt
	kts		deg		deg	rad	cm/s	cm/s
1	20	1.9815	195	1.51	-68.4	2.20959	2.4020821	-1.784
2	20	1.9815	195	1.62	36	4.03171	-2.4946619	-2.02
3	20	1.9815	195	1.76	140.4	5.85383	-1.4517543	3.1709
4	20	1.9815	195	1.94	-115.4	1.38928	3.7809569	0.6939
5	20	1.9815	195	2.19	-11.7	3.19919	-0.2497982	-4.332
6	20	1.9815	195	2.54	91.3	4.99688	-4.8307096	1.4126
7	20	1.9815	195	3.29	192	6.75442	2.9596254	5.8086
8	20	1.9815	195	5.62	281.4	8.31475	9.974673	-4.951
sum							10.090413	-2.002
							v=	10.287
angle(deg)								-78.78

Surface Layer								
t	Ft	Stress	theta-t	Kt	phi-t	th+phi-t	Ut	Vt
	kts		deg		deg	rad	cm/s	cm/s
1	18	1.605015	195	1.51	-68.4	2.20959	1.9456865	-1.445
2	18	1.605015	195	1.62	36	4.03171	-2.0206761	-1.636
3	18	1.605015	195	1.76	140.4	5.85383	-1.175921	2.5684
4	18	1.605015	195	1.94	-115.4	1.38928	3.0625751	0.5621
5	18	1.605015	195	2.19	-11.7	3.19919	-0.2023366	-3.509
6	18	1.605015	195	2.54	91.3	4.99688	-3.9128748	1.1442
7	18	1.605015	195	3.29	192	6.75442	2.3972965	4.705
8	18	1.605015	195	5.62	281.4	8.31475	8.0794852	-4.011
sum							8.1732348	-1.621
							v=	8.3325
angle(deg)								-78.78

Surface Layer								
t	Ft	Stress	theta-t	Kt	phi-t	th+phi-t	Ut	Vt
	kts		deg		deg	rad	cm/s	cm/s
1	22	2.397615	195	1.51	-68.4	2.20959	2.9065193	-2.159
2	22	2.397615	195	1.62	36	4.03171	-3.0185408	-2.444
3	22	2.397615	195	1.76	140.4	5.85383	-1.7566227	3.8368
4	22	2.397615	195	1.94	-115.4	1.38928	4.5749579	0.8397
5	22	2.397615	195	2.19	-11.7	3.19919	-0.3022559	-5.242
6	22	2.397615	195	2.54	91.3	4.99688	-5.8451587	1.7092
7	22	2.397615	195	3.29	192	6.75442	3.5811467	7.0284
8	22	2.397615	195	5.62	281.4	8.31475	12.069354	-5.991
sum							12.2094	-2.422
							v=	12.447
angle(deg)								-78.78

Figure I-3. Local wind driven current, 10% speed perturbation at +15°direction.

Surface Layer								
t	Ft	Stress	theta-t	Kt	phi-t	th+phi-t	Ut	Vt
	kts		deg		deg	rad	cm/s	cm/s
1	19.46	1.875944	180	1.51	-68.4	1.94779	2.6337543	-1.043
2	19.46	1.875944	180	1.62	36	3.76991	-1.7862961	-2.459
3	19.46	1.875944	180	1.76	140.4	5.59203	-2.1045577	2.544
4	19.46	1.875944	180	1.94	-115.4	1.12748	3.2875356	1.561
5	19.46	1.875944	180	2.19	-11.7	2.93739	0.8331143	-4.023
6	19.46	1.875944	180	2.54	91.3	4.73508	-4.7636701	0.1081
7	19.46	1.875944	180	3.29	192	6.49262	1.2832006	6.037
8	19.46	1.875944	180	5.62	281.4	8.05295	10.334805	-2.084
sum							9.7178865	0.6419
							v=	9.7391
angle(deg)								86.221

(1kt = 0.5144444 m/s—above result for wind speed of 10 m/s)

Figure I-4. Local wind driven current: comparison with Dick (1991).